Non-ideal GRMHD and Compact Objects

Luca Del Zanna

Dipartimento di Fisica e Astronomia, Università degli Studi di Firenze

INAF - Osservatorio Astrofisico di Arcetri

INFN - Sezione di Firenze

luca.delzanna@unifi.it

SIGRAV 2023 - Trieste

BNS merger events and short GRBs

August 2017: a binary neutron star merger gives birth to multimessenger astrophysics, and confirms that short GRBs and their jets are produced by these events.

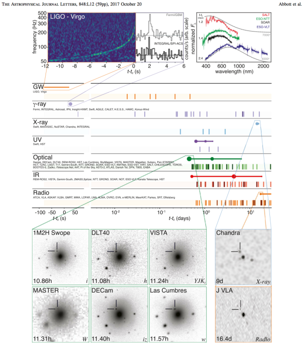

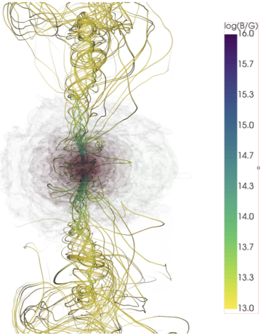

A dynamically important magnetic field is crucial for launching/collimation of GRB jet and for kilonova properties (Ciolfi 2020), but important questions are still unanswered:

- can the remnant be long-lived (at least 10 ms) before eventual collapse to a BH?
- how is the magnetic field increased from $B \sim 10^{10-12}$ G up to 10^{15-16} G?

Long-lived BNS merger remnants

Several fates for a BNS merger remnant are possible (Sarin & Lasky 2021), the most natural being a rotating BH powering a short GRB jet of case C (Rezzolla et al. 2011).

Depending on mass and spin, the most intriguing case is F: a supramassive NS supported by strong differential rotation, living in a meta-stable phase from 10 to 10^5 s.

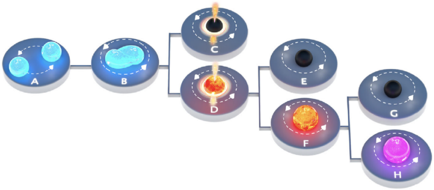

Short GRB X-ray lightcurves often show a persistent plateau (Rowlinson et al. 2010, 2013). The spindown of a millisecond rotating remnant with magnetar-like fields of 10^{15-16} G (case F) could be the engine (Metzger et al. 2011, Bucciantini et al. 2012)!

Magnetic amplification by $\sim 10^2 - 10^3$ could be gained during the merger (phase B) via Kelvin-Helmholtz instabilities (Price & Rosswog 2006, Kiuchi et al. 2015), followed by MRI (phase D) as for core-collapse magnetars (Moesta et al. 2015; Reboul-Salze et al. 2021).

However, global 3D simulations resolving MRI are computationally challenging, some sub-grid modeling is required (Giacomazzo et al. 2015). GRMHD *mean-field dynamo* ?

Field amplification in compact objects

The mean-field dynamo mechanism from classical to relativistic MHD

Within classical MHD consider small-scale turbulent fluctuations in the fields $\boldsymbol{v}$ e $\boldsymbol{B}$:

$$\boldsymbol{v}(\boldsymbol{x},t) = \boldsymbol{v}_0(\boldsymbol{x},t) + \delta\boldsymbol{v}(\boldsymbol{x},t), \quad \boldsymbol{B}(\boldsymbol{x},t) = \boldsymbol{B}_0(\boldsymbol{x},t) + \delta\boldsymbol{B}(\boldsymbol{x},t)$$

The resistive induction equation for *correlated* fluctuations may be written as

$$\partial_t \boldsymbol{B}_0 = \boldsymbol{\nabla} \times (\boldsymbol{v}_0 \times \boldsymbol{B}_0) + \eta_r \nabla^2 \boldsymbol{B}_0 + \boldsymbol{\nabla} \times \boldsymbol{\mathcal{E}}$$

$$\boldsymbol{\mathcal{E}} = \langle \delta\boldsymbol{v} \times \delta\boldsymbol{b} \rangle \simeq \alpha_{dyn} \boldsymbol{B}_0 - \beta_{dyn} \boldsymbol{\nabla} \times \boldsymbol{B}_0$$

$$\Downarrow$$

$$\partial_t \boldsymbol{B} = \boldsymbol{\nabla} \times (\boldsymbol{v} \times \boldsymbol{B}) + \alpha_{dyn} \boldsymbol{\nabla} \times \boldsymbol{B} + (\eta_r + \beta_{dyn}) \nabla^2 \boldsymbol{B}$$

or equivalently, is like assuming a generalized Ohm's law ($\xi \equiv -\alpha_{dyn}, \eta = \eta_r + \beta_{dyn}$)

$$\boxed{\boldsymbol{E}' \equiv \boldsymbol{E} + \boldsymbol{v} \times \boldsymbol{B} = \eta \boldsymbol{J} + \xi \boldsymbol{B}}$$

A fully covariant formulation of Ohm's law for plasmas with finite resistivity and mean-field dynamo action was proposed by Bucciantini & Del Zanna (2013):

$$\boxed{e^\mu = \eta j^\mu + \xi b^\mu}$$

where e^μ, b^μ and j^μ are measured in the fluid comoving frame.

The $\alpha - \Omega$ dynamo and the solar cycle

In the interior of stars, differential rotation and fully developed turbulence lead to exponentially growing $\alpha - \Omega$ dynamo modes, damped by resistivity (Parker 1955):

$$\boldsymbol{B}_P \Rightarrow \boldsymbol{B}_T \Rightarrow \boldsymbol{B}_P \Rightarrow \dots$$

- Differential rotation $\Rightarrow$ generation of toroidal field (Ω effect)
- Toroidal field $\Rightarrow$ generation of poloidal field (α effect)

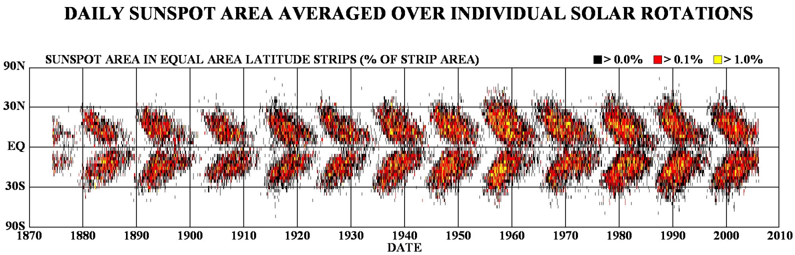

The mechanism accounts for the solar 11 years cycle and for the *butterfly diagram*.

The same behavior is expected in GRMHD, conservative formalism for $3 + 1$ metrics and numerical high-order (implicit-explicit) methods in Del Zanna and Bucciantini (2018).

The ECHO code: first application of GRMHD dynamo in accretion disks

The resistive-dynamo model is implemented in the ECHO (Eulerian Conservative High-Order) code for 3 + 1 GRMHD (Del Zanna et al. 2007).

The first application has been for accretion disks around black holes (Bugli et al. 2014, Tomei et al. 2020, 2021): the magnetic field necessary to reproduce EHT observations (SANE-type) can be reached in small times, not related with the disk's rotation period.

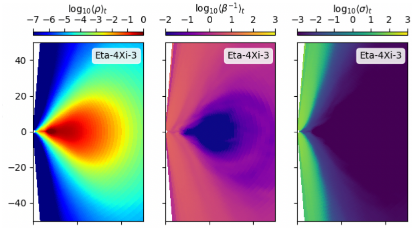

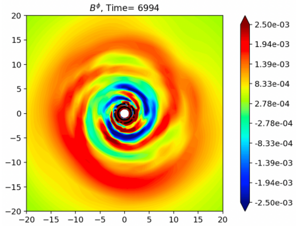

The expected pattern of an equatorial cusp and a polar magnetized outflow is reproduced, even by starting with initial negligible fields.

3D simulations: spiral-like dynamo waves of alternating polarity (Del Zanna et al. 2022).

Dynamo amplification in neutron stars: test on XNS equilibrium

For neutron stars, the GRMHD dynamo was first tested on equilibrium configurations (generalized Bernoulli and Einstein equations) in axisymmetric conformally flat metric.

The XNS freely downloadable numerical tool (Bucciantini & Del Zanna 2011) finds neutron star equilibria in GRMHD, including magnetic fields, differential rotation, tabulated EoSs, and extended gravities (www.arcetri.inaf.it/science/ahead/XNS).

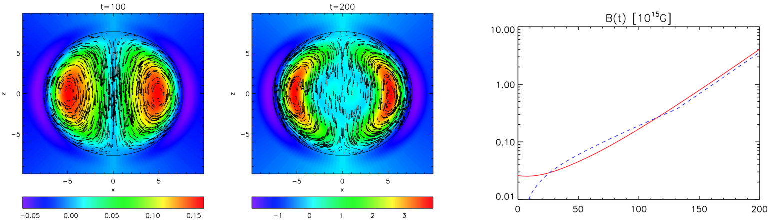

Dynamo test: exponential amplification of both toroidal and poloidal field components, with the expected growth rate (here for a static star, hence α^2-dynamo):

$$\gamma \sim \alpha_{\rm dyn}/\lambda, \quad \alpha_{\rm dyn} = |\xi|, \quad \lambda \sim |\boldsymbol{B}|/|\nabla \boldsymbol{B}$$

This was however a toy model with uniform ξ and η. They should be present where turbulence is fully developed by some mechanism.

Dynamo amplification in neutron stars: systematic investigation

Several (kinematic) runs performed in (Franceschetti et al. 2020), $4 - 5$ ms typically enough for a factor 1000 of amplification (local quenching for $B \sim 10^{15}$ G).

Linear dependence of exponential growth rate with the dynamo parameter ξ.

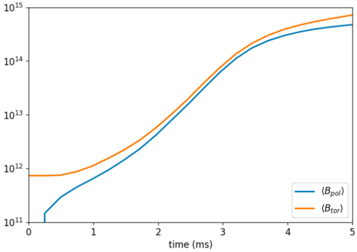

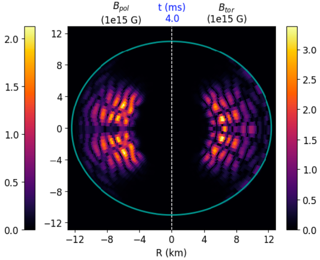

Here differential rotation present (Ω-dynamo), with turbulent action (α-dynamo) only in the outer layer where *neutron-finger instability* operates (Bonanno, Rezzolla, Urpin 2003).

Different choices of ξ and η profiles are of course possible...

Dynamo amplification in BNS remnants from 3D simulations

Numerical relativity 3D simulations show that after the inspiral and merger of two magnetized NS a meta-stable remnant may indeed form.

The rotation profile $\Omega(r)$ is never monotonic: centrally flat, then a sharp rise up to a maximum, and Keplerian-like decay.

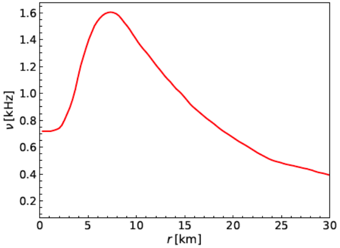

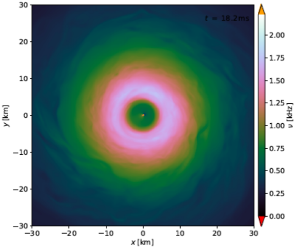

Using data from 3D BNS simulations by Kalinani and Ciolfi we applied the kinematic GRMHD dynamo on top of a remnant (with $\Omega_0 = 0.72$ kHz and $\Omega_{max} = 1.60$ kHz).

Dynamo amplification in BNS remnants from 3D simulations

Dynamo more active where gradients of Ω are stronger, after the central plateau. For this case we have used the following profiles:

$$\xi = \xi_0 \frac{\rho}{\rho_c} \sin 2\theta, \qquad \eta = \eta_0 \frac{\rho}{\rho_c}$$

with $\xi_0 = 10^{-2}$ and $\eta_0 = 10^{-3}$ (here $\alpha - \Omega$ dynamo with weak migrating islands).

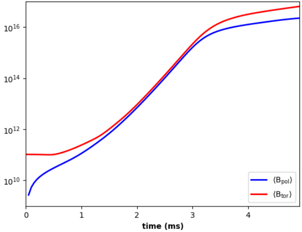

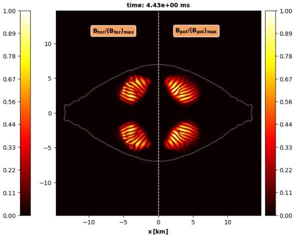

In the case with strongest dynamo, a short timescale of 1 ms is typically found for each decade of amplification (local quenching for $B \sim 10^{17}$ G) (Del Zanna et al 2022).

We find both $\alpha - \Omega$ and α^2 regimes depending on Reynolds-like dynamo numbers:

$$C_\xi \simeq \frac{R_m \xi_0}{\eta_0}, \qquad C_\Omega \simeq \frac{R_m^2 \Delta\Omega}{\eta_0}$$

Dynamo amplification in BNS remnants from 2D XNS equilibria

Instead of running computationally heavy 3D numerical relativity simulations of BNS inspiral and merging, we use axisymmetric equilibria obtained with the XNS tool, recently updated to remnant's $\Omega(r)$ profiles (Franceschetti et al. 2022).

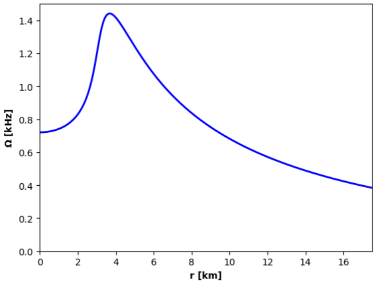

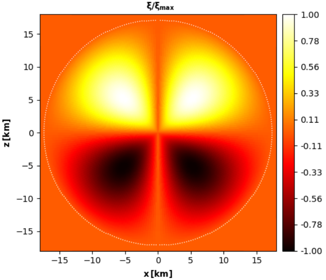

Above are the rotation profile $\Omega(r)$ arising from a particular choice of $\Omega(j)$, and the adopted 2D distribution of $\xi(r,\theta)$. The star has $M_0 = 2.78 M_\odot$ and $R = 17.5$ km.

The distribution of nascent and evolving magnetic islands is localized where the profile of Ω is stronger and more rapidly decreasing and ξ is higher. Work still in progress...

Resistive astrophysical jets

Axisymmetric jets with uniform resistivity

We are also interested in the possible role of resistivity in the context of short GRB jets emerging from BNS merger events. Both the jet and the ambient are expected to be magnetized and turbulent.

Resistivity is not provided by collisions, rather by (sub-grid) turbulence, as the dynamo.

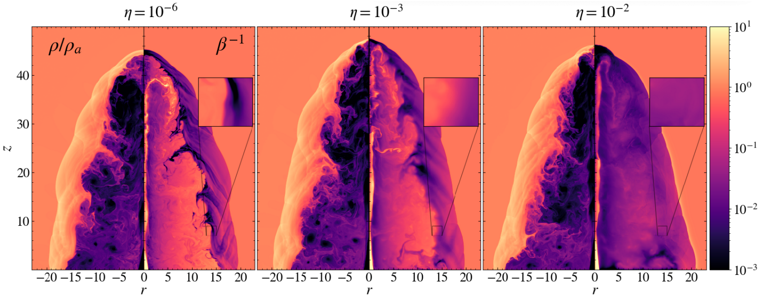

Here the jet is relativistic with Lorentz $\Gamma = 10$ and highly magnetized, threaded by both poloidal and toroidal fields. The ambient in uniform, with a vertical magnetic field.

A resistivity coefficient above $\eta \simeq 10^{-3}$ clearly diffuses the electromagnetic structures, magnetization is strongly reduced in the jet plasma.

Axisymmetric jets with uniform resistivity

The electromagnetic energy contained in the injected plasma is heavily affected by the value of η, though the overall jet dynamics is not.

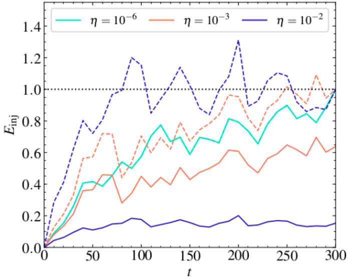

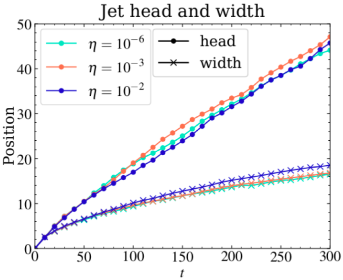

The overall Ohmic-type dissipated power can be also computed, in the comoving frame the covariant definition is

$$\mathcal{P} = j_\mu e^\mu = \eta j^2$$

this is enhanced for increasing values of η, as expected (even if currents are stronger when smearing is less important).

Axisymmetric jets with variable resistivity

With a (high) resolution of 48 cells per injection radius ($r_j = 1$ in code units), the estimated numerical resistivity is $\eta \sim 10^{-4}$.

To preserve turbulent thin current sheets (optimal sites for fast reconnection), we propose two (more realistic?) models with variable resistivity η:

- Tr-case, given a passive tracer f (1 at injection, 0 outside), $\eta = \max(10^{-6}, 10^{-3} f)$
- S-case: given a constant Lundquist number $S = 10^3$, $\eta = v_A r_j / S$

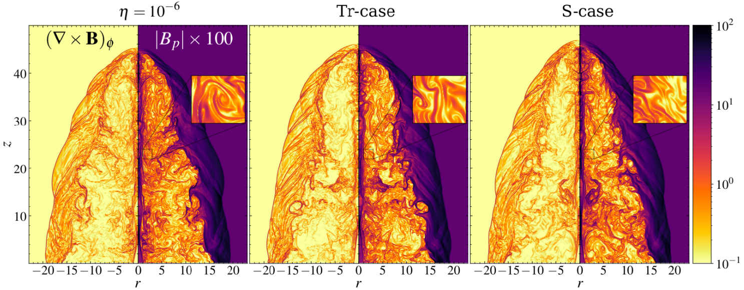

More details about results can be found in a paper recently accepted for A&A, written in collaboration with the Padova and Torino groups (Mattia, Del Zanna et al. 2023).

Summary

Non-ideal effects are commonly neglected in relativistic hydro/MHD simulations, here we have presented the theory relevant for numerical simulations and a few applications:

A unified set of equations for resistive-dynamo relativistic MHD has been derived in both covariant and $3+1$ form, valid for any curved manifold, ready for numerical integration (Bucciantini & Del Zanna 2013, Del Zanna & Bucciantini 2018).

Our GRMHD model for the mean-field dynamo has been applied to accretion disks around Kerr black holes, to neutron stars and to BNS meta-stable hypermassive merger remnants (Del Zanna et al. 2022).

The first systematic study of the importance of physical resistivity in simulations of propagating relativistic jets has been performed (Mattia, Del Zanna et al. 2023), extension to the case of GRB jets from BNS merger is under investigation.

Thank you!